Engineering an Antibiotic to Fight Cancer: Optimization of the Novobiocin Scaffold to Produce Anti-proliferative Agents

Huiping Zhao,[†,⊥] Alison C. Donnelly,[†,⊥] Bhaskar R. Kusuma,[†,⊥] Gary E. L. Brandt,[†] Douglas Brown,[‡] Roger A. Rajewski,[§] George Vielhauer,[‖] Jeffrey Holzbeierlein,[‖] Mark S. Cohen,[‖] and Brian S. J. Blagg*,[†]

[†]Department of Medicinal Chemistry, The University of Kansas, 1251 Wescoe Hall Drive, Malott 4070, Lawrence, Kansas 66045-7563, United States

[‡]Biotechnology Innovation & Optimization Center, The University of Kansas, 2099 Constant Avenue, Lawrence, Kansas 66047-2535, United States

[§]Department of Pharmaceutical Chemistry, The University of Kansas, 2095 Constant Avenue, Lawrence, Kansas 66047-2535, United States

[‖]Department of Urology, The University of Kansas Medical Center, 3901 Rainbow Boulevard, Mail Stop 3016, Kansas City, Kansas 66160, United States

Ⓢ Supporting Information

ABSTRACT: Development of the DNA gyrase inhibitor, novobiocin, into a selective Hsp90 inhibitor was accomplished through structural modifications to the amide side chain, coumarin ring, and sugar moiety. These species exhibit ∼700-fold improved anti-proliferative activity versus the natural product as evaluated by cellular efficacies against breast, colon, prostate, lung, and other cancer cell lines. Utilization of structure—activity relationships established for three novobiocin synthons produced optimized scaffolds, which manifest midnanomolar activity against a panel of cancer cell lines and serve as lead compounds that manifest their activities through Hsp90 inhibition.
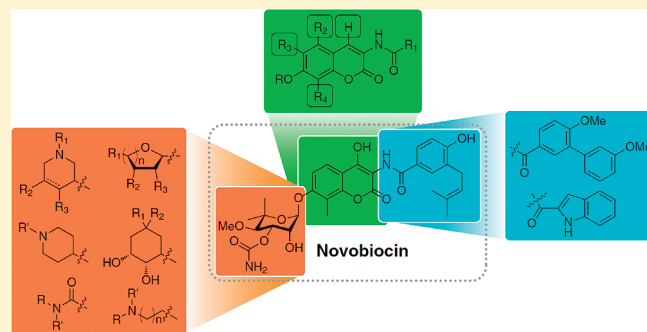
■ INTRODUCTION

The Hsp90 molecular chaperone has emerged as a promising target for the treatment of cancer.[1] While most current therapies are directed at disrupting a single molecular function, Hsp90 is distinctive as it serves to modulate multiple oncogenic pathways. Moreover, Hsp90 is overexpressed in human malignancies and its inhibition provides a unique opportunity to develop small molecules that exhibit high differential selectivity.[1−4] There are more than 150 client proteins dependent upon Hsp90 for their folding and conformational maintenance, many of which contribute to cancer cell proliferation and growth.[5−12] Small molecule Hsp90 inhibitors transform the normal protein folding machinery into a catalyst for protein degradation via utilization of the ubiquitin—proteasome pathway.[13,14] As such, Hsp90 inhibition is similar to a combinatorial attack, in which multiple signaling pathways that contribute to malignancy are simultaneously disrupted.[1,2,15−17]

Novobiocin (Figure 1), a member of the coumermycin family of antibiotics, manifests potent antimicrobial activity through inhibition of DNA gyrase-mediated ATP-hydrolysis.[18−22] Co-crystal structures of DNA gyrase B bound to novobiocin and ADP revealed both molecules to bind in an atypical, bent conformation.[23−25] It was this unique binding conformation
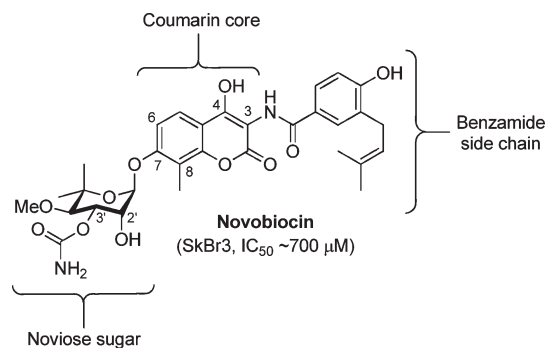

Figure 1. Structure of novobiocin.

that led Neckers and co-workers to hypothesize that novobiocin exhibits its antitumor activity (∼700 μM) against SKBr3 breast cancer cells through Hsp90 inhibition. Through subsequent Western blot analyses, Neckers and co-workers confirmed that novobiocin induces degradation of Hsp90-dependent clients in a concentration-dependent manner, a hallmark of Hsp90

inhibition. In contrast to other Hsp90 inhibitors, it was shown that novobiocin bound to the C-terminus, revealing a previously unrecognized binding site, and perhaps, a new opportunity to modulate the Hsp90 protein folding machinery.[26]

Although no cocrystal structure of Hsp90 bound to C-terminal inhibitors has been reported, the structure and function of the Hsp90 C-terminal nucleotide binding site are under intense investigation. Compounds exhibiting higher affinity for Hsp90 than novobiocin are likely to provide the tools necessary for elucidation of the Hsp90 C-terminal nucleotide-binding pocket and provide new Hsp90 modulators that manifest chemotherapeutic potential.[27] The poor Hsp90 inhibitory activity of novobiocin[26] has been greatly improved upon by the preparation of analogues. Yu and co-workers produced a library of compounds that established the first structure—activity relationships for novobiocin as an Hsp90 inhibitor. This focused library explored essential features of the benzamide side chain, coumarin core, and noviose sugar, highlighting that attachment of noviose to the 7-position and an amide linker at the 3-position of the coumarin ring are critical for Hsp90 inhibitory activity. Moreover, modifications to the sugar identified the diol as most potent versus the cyclic carbonate and corresponding carbamates as found in novobiocin.[28]
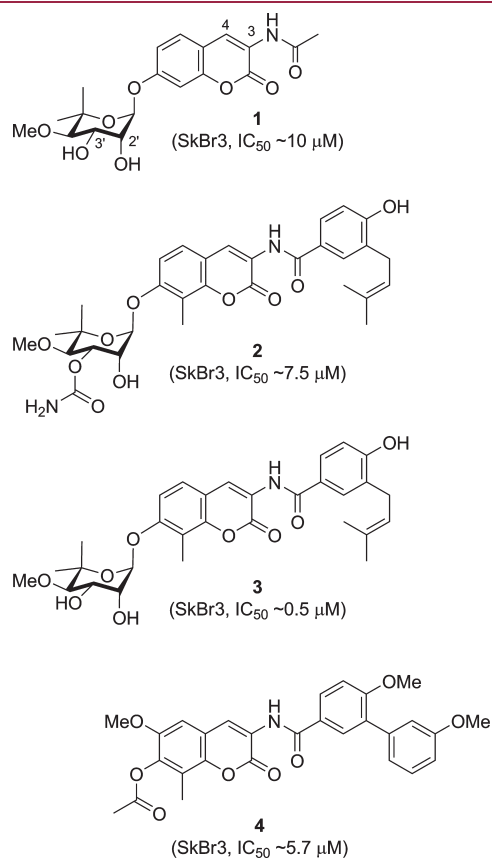

Figure 2. Structures of 1, 2, 3, and 4.[28−30]

Compound 1 (Figure 2) was the most notable compound identified from this library. 1, with a shortened N-acyl side chain, a 4-deshydroxy substituent and no carbamoyl group on noviose, induced degradation of Hsp90-dependent client proteins at ~70-fold lower concentration than novobiocin.[28] However, in contrast to N-terminal inhibitors, 1 induced Hsp90 at concentrations

1000−10000-fold lower than that required for client protein degradation, a phenomenon that had not been previously observed. Because of its activity and nontoxic nature, 1 was evaluated as a neuroprotective agent and produced an EC_{50} of 6 nM in a culture model for Alzheimer's disease.[28]

To confirm SAR trends observed by Yu and co-workers, two natural product analogues, 2 and 3 (Figure 2), were designed and subsequently evaluated by Burlison and co-workers. This study aimed at elucidating functionalities on novobiocin that are responsible for DNA gyrase inhibition and to deconvolute Hsp90-selective inhibitory compounds. Studies with these compounds confirmed that the 4-hydroxyl and the 3′-carbamate are detrimental to Hsp90 inhibitory activity but critical for DNA gyrase inhibition.[29] This study confirmed the trends observed from a library based on compound 1, and produced the first selective inhibitors of the Hsp90 C-terminus.
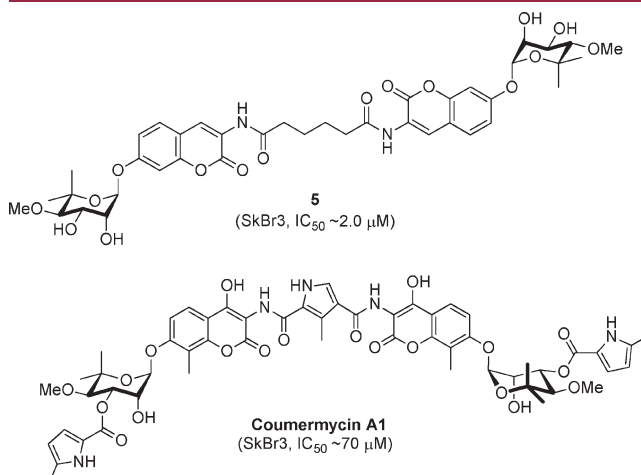

Figure 3. Structures of 5 and coumermycin A1.

On the basis of the cytotoxicity of coumermycin A1 (Figure 3), another member of the coumermycin family of antibiotics, it appeared that dimerization could increase Hsp90 inhibitory activity. Burlison and co-workers dimerized 1 in an attempt to transform a nontoxic agent into a more potent analogue. The resulting compound, 5, the most potent identified, exhibited low micromolar anti-proliferative activity but did not induce the heat shock response. These results suggested that modification of the amide side chain could convert a nontoxic molecule into an anti-proliferative agent.[31] Consequently, a series of monomeric species based on 5 was synthesized and evaluated in cell proliferation studies.[32] Monomeric analogues were designed to include biaryl and heterocyclic amide derivatives that explored hydrogen-bonding interactions within the putative binding pocket that typically accommodates the prenylated benzamide of novobiocin. This library identified key functionalities and established the first set of SAR for the amide side chain (Figure 4).

The coumarin core of novobiocin was recently explored and SAR established. Derivatives of 1 with variations to the coumarin ring were designed to probe the importance of interactions manifested by the natural substrate purine ring as well the size and nature of the novobiocin binding pocket. The 6- and 8-positions of the coumarin scaffold proved tolerable to substitution, and incorporation of alkoxy groups at these locations led to improved inhibitory activity. Moreover, the lactone moiety of the coumarin ring was found to be dispensable (Figure 5).[33]
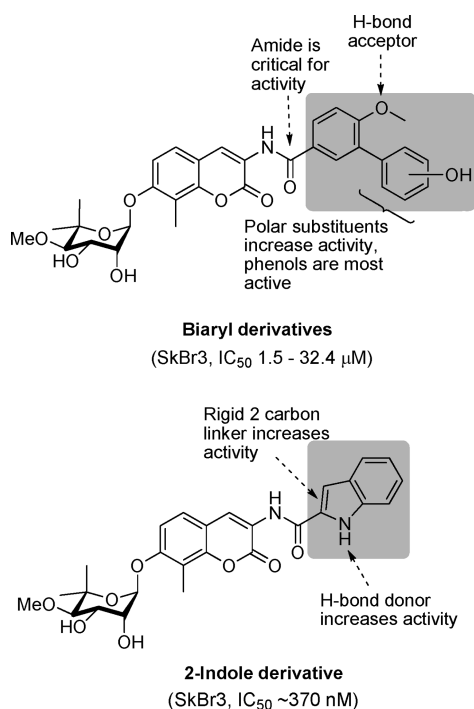
Figure 4. Benzamide SAR.[32]
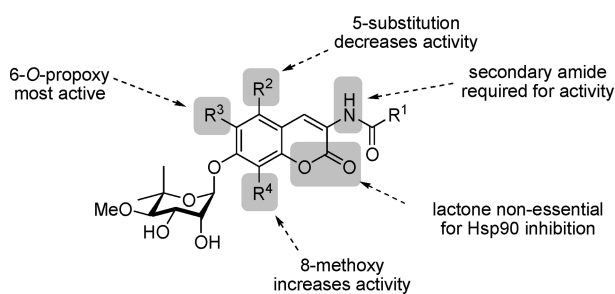
Figure 5. Coumarin SAR.[33]

Renoir and co-workers examined the role of noviose in Hsp90 inhibition. Their structure—activity relationship studies demonstrated that Hsp90 inhibition was observed by analogues that lack the noviose moiety if a tosyl substituent is attached to the C-4 or C-7 position of the coumarin. These analogues manifested mid-micromolar IC$_{50}$ values.[34] In a subsequent paper, the same group suggested that Hsp90 inhibition can be enhanced by removal of C7/C8 substituents in denoviose analogues bearing a tosyl group at the 4-position. These studies produced inhibitors with simplified coumarins that also exhibited mid-micromolar IC$_{50}$ values.[35] The compounds produced in these two publications represented the first novobiocin analogues that lacked the noviose sugar while manifesting Hsp90 inhibition.

The noviose sugar found in novobiocin is complex and is prepared via laborious efforts. Even the most efficient syntheses of noviose require more than 10 steps and the overall yields are less than optimal.[36] In an effort to gain further insight into this region of novobiocin, simplified noviose derivatives were attached to the novobiocin core. This study, which resulted in compounds that exhibit a 700-fold improvement in activity over novobiocin, indicated that while the sugar moiety plays a critical role in maintaining binding interactions with Hsp90, not all functionalities are necessary.

Sugar mimics were originally attached to the 7-position of coumarin containing an 8-methyl substituent and a biaryl benzamide. The most potent coumarin scaffolds obtained from the coumarin studies were coupled with the optimal biaryl side chain to yield a scaffold upon which sugar surrogates were appended.[32,33] On the basis of the inhibitory activity manifested by the biaryl analogues, the most promising sugar surrogates were coupled with coumarins containing the 2-indole side chain.[32] The simplified sugars and related azasugars were found to conserve structural units present in noviose but lacked the complexity of multi-step synthesis. These sugar surrogates were designed to probe potential hydrogen bonds as well as to determine the dimensions of the pocket. In addition to simplified sugars, several surrogates containing heteroatoms and various appendages were also explored. These diverse sugar and nonsugar analogues simplify the preparation of novobiocin analogues while providing a handle to improve both solubility and efficacy. The design, synthesis, and biological evaluation of these optimized compounds are reported herein.

■ RESULTS AND DISCUSSION

Design, Synthesis, and Evaluation of Modified Sugar Analogues of Novobiocin. Numerous biologically active natural products contain carbohydrates appended to their scaffolds that serve to increase solubility and provide interactions with their cognate receptor. In many cases, removal of the carbohydrate moiety renders the aglycon inactive, whereas alteration of the sugar ring size can alter affinity of the compounds toward specific targets.[37−39] Modifications to the noviose pyranose ring were proposed to elucidate functionalities required for inhibitory activity as well as to determine whether different sized sugars can be utilized as replacements for noviose. Thus, five-, six-, and seven-membered sugars were synthesized and coupled to the aforementioned scaffolds to determine optimal interactions. When available, the α- and β-anomers were also evaluated. A set of protected mono-, di- and trihydroxylated furanoses, pyranoses, and oxepanose sugars previously synthesized by Yu and co-workers[40] (**E−L**, Figure 6) was chosen based on these considerations.
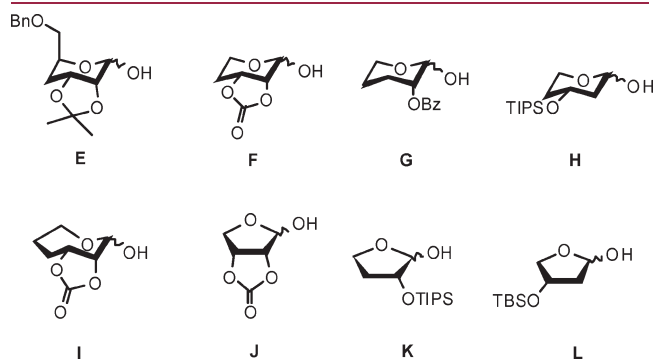

Figure 6. Five-, six-, and seven-membered noviose alternatives.

The analogues were assembled in modular fashion, allowing sequential coupling of sugars and the biaryl acid side chain with the desired scaffold. As shown in the retrosynthetic analysis (Scheme 1), the biaryl acid side chain was assembled through a Suzuki coupling reaction, as described previously.[33] Next, the

Scheme 1. Retrosynthesis of Novobiocin Biaryl Analogues with Sugars E−L

6a: X = H, Y = CH₃
6b: X = H, Y = OCH₃
6c: X = OMe, Y = Me
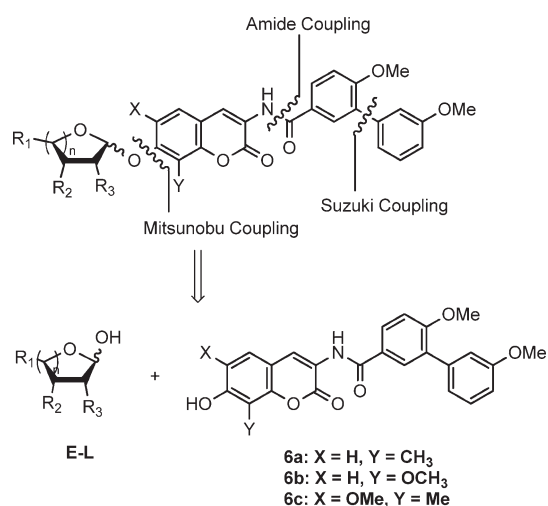
biaryl acid was converted to its corresponding acid chloride and then coupled with the protected coumarin, **9**. Finally, Mitsunobu etherification between coumarin phenols **6a−c** and sugars **E−L** yielded the desired analogues in good yields.

Synthesis of these analogues, as described in Scheme 2, began via protection of phenol **7**[32,33] as the corresponding ester, **8**. Next, hydrogenolysis was employed to liberate vinylogous amide **9**, which was subsequently coupled with biaryl acyl chloride, **11**. The biaryl acid chloride was generated from the corresponding biaryl acid **10**, as described previously.[33] Finally, solvolysis of ester **12** afforded phenol **6a−c** in good yield.

Coumarin phenols **6a−c** and protected sugar **F** were coupled via a Mitsunobu etherification to yield an inseparable mixture of diastereomers, **13**, in a 3:2 ratio, respectively (Scheme 3). The cyclic carbonates of the resulting mixture were solvolyzed to afford a mixture of diols **14** and **15**, which were separated by silica chromatography. The stereochemistry at the anomeric carbon was assigned by 2D-NOESY spectroscopy.

An anomeric mixture of compound **13** was synthesized via Mitsunobu etherification between sugar **F** and coumarin **6**.

Scheme 2. Synthesis of Phenol 6
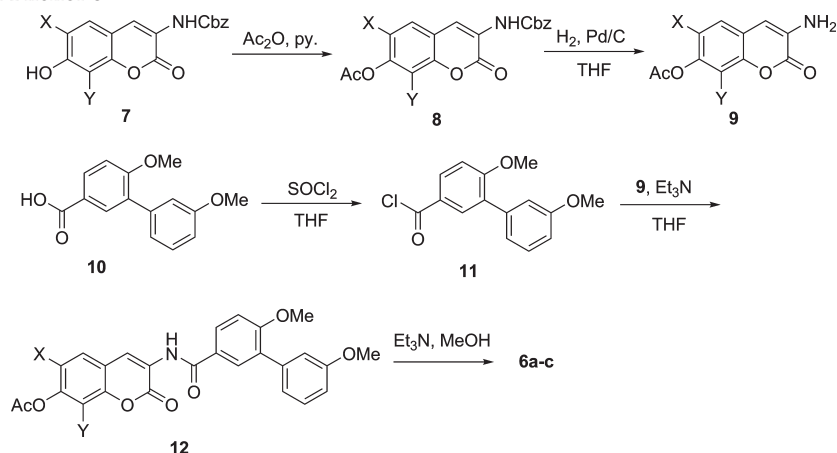
Scheme 3. Synthesis of Pyranose-Containing Biaryl Analogues
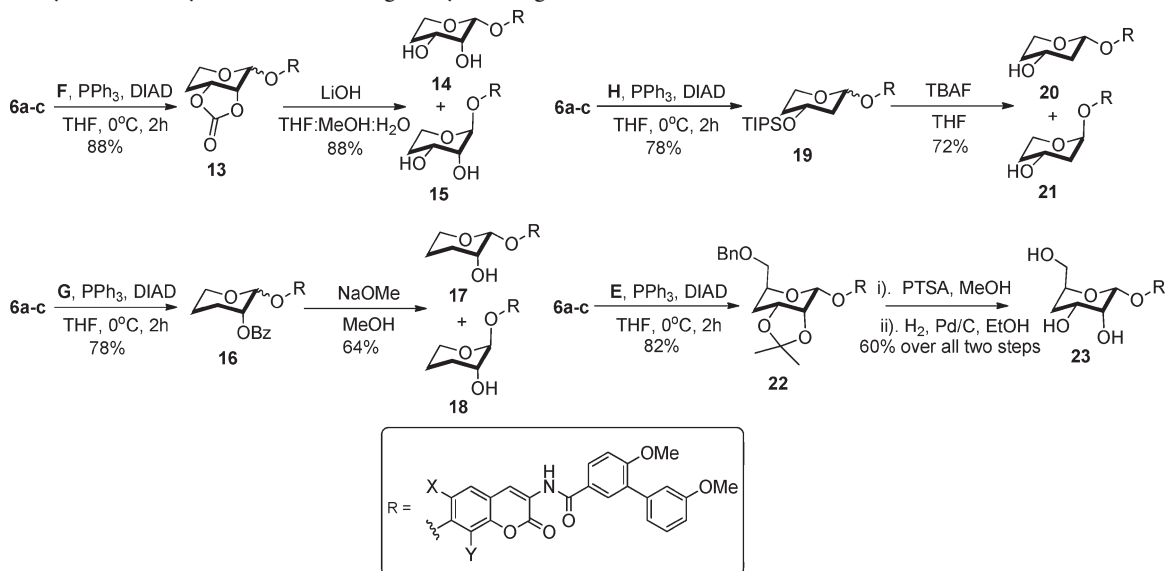
Scheme 4. Synthesis of Furanose- and Oxepanose-Containing Biaryl Analogues
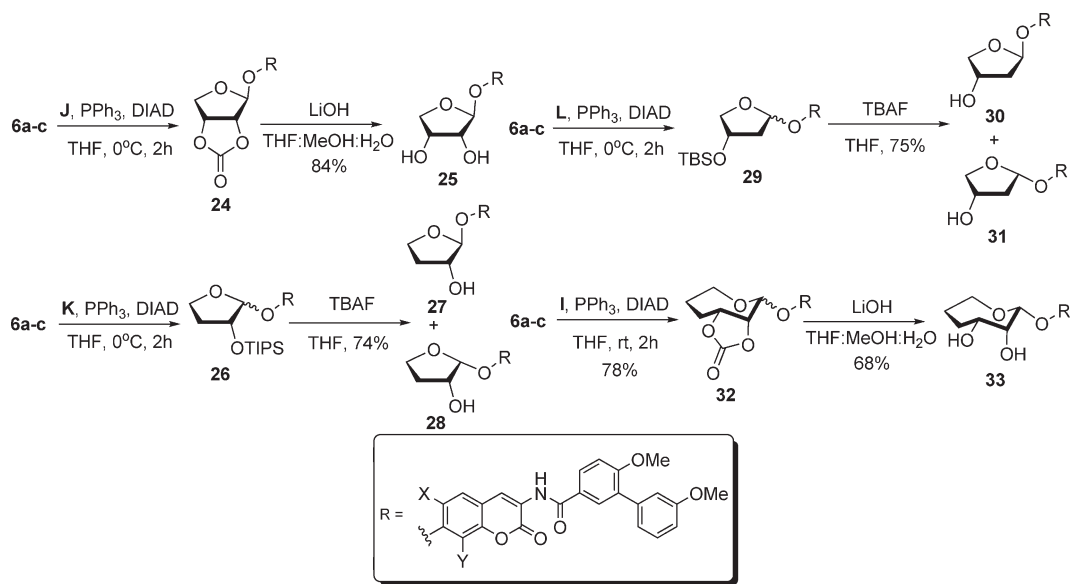
Scheme 5. Synthesis of Cyclohexyl-Containing Biaryl Analogues

Likewise, the Mitsunobu conditions were used to append sugar **G** to coumarin **6** and furnish the anomeric mixture of compound **16** and to attach sugar **H** to coumarin **6** to yield anomeric mixture **19**. Solvolysis of the cyclic carbonate present in **13** furnished a mixture of separable diols, **14** and 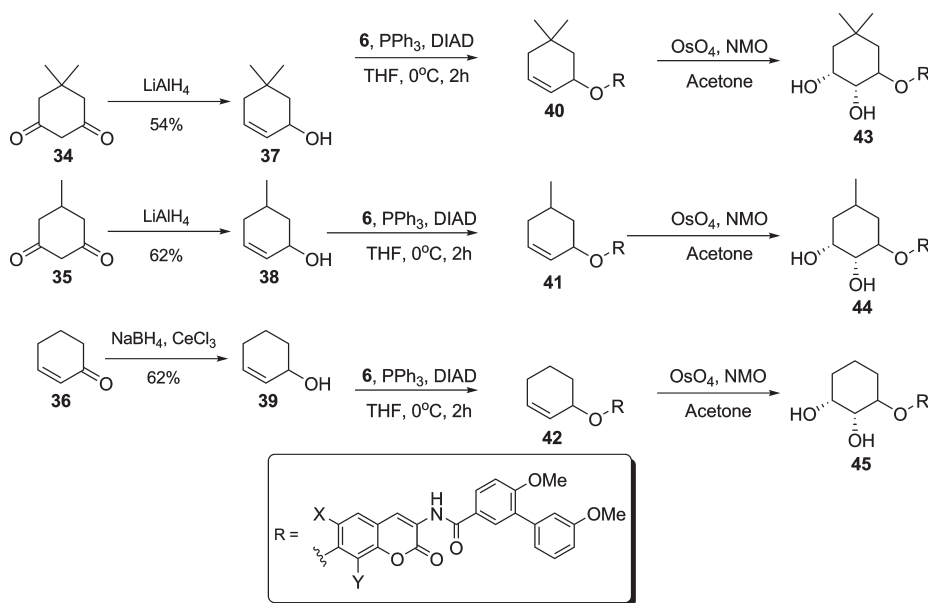**15**. Moreover, benzoyl (Bz) deprotection of **16** yielded analogues **17** and **18** in a 3:2 ratio,[5] while TIPS removal of **19** furnished analogues **20** and **21** in a 4:3 ratio. Not surprisingly, a single diastereomer of **22** was exclusively formed when coumarin **6** and protected sugar **E** were subjected to Mitsunobu conditions. Subsequent deprotection of the acetonide and benzyl protecting groups afforded triol **23** in good yield (Scheme 3).

As shown in Scheme 4, protected furanose sugars **J**−**L** were coupled with coumarin **6** by enlisting Mitsunobu etherification to afford the corresponding analogues in good yields. Mitsunobu coupling of protected sugar **J** with coumarin **6** yielded exclusively diastereomer **24**, which was subsequently hydrolyzed to afford diol **25**. Mitsunobu etherification was used to append sugar **K** to yield analogue **26**, which, after silyl removal, furnished separable compounds **27** and **28**. Likewise, the same conditions were applied to append sugar **L** to **29**, which, after silyl cleavage, yielded analogues **30** and **31**. Protected oxepanose **I** was coupled to coumarin **6** using Mitsunobu conditions to afford **32** as the major product, which was hydrolyzed to give **33**.

Table 1. Anti-proliferative Activity of Various Sugar Analogues
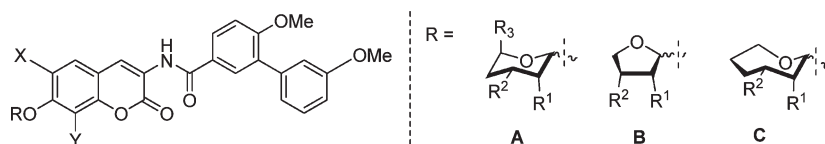
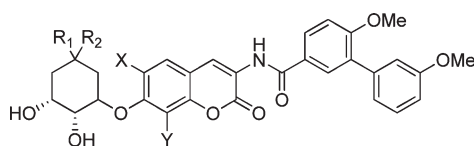| compd (IC$_{50}$, μM)	R	R^1	R^2	R^3	anomer	X	Y	SKBr3	MCF-7	LNCAP-LN3	PC3-MM2
14a	A	OH	OH	H	β	H	CH$_3$	6.23 ± 0.52[a,c]	2.56 ± 0.08[a]	3.59 ± 3.40[b]	NT[b]
15a	A	OH	OH	H	α	H	CH$_3$	6.71 ± 0.80	42.56 ± 2.48	1.20 ± 0.83	12.88 ± 9.30
14b	A	OH	OH	H	β	H	OCH$_3$	1.46 ± 0.46	17.46 ± 1.22	2.29 ± 1.25	10.72 ± 10.85
15b	A	OH	OH	H	α	H	OCH$_3$	11.10 ± 0.43	10.85 ± 0.18	NT	NT
14c	A	OH	OH	H	β	OCH$_3$	CH$_3$	7.18 ± 0.20	9.50 ± 0.16	12.76 ± 5.12	24.03 ± 17.14
15c	A	OH	OH	H	α	OCH$_3$	CH$_3$	12.52 ± 0.54	64.51 ± 3.52	14.93 ± 9.24	25.37 ± 7.26
17a	A	OH	H	H	β	H	CH$_3$	>100	>100	3.75 ± 0.01[d]	10.05 ± 0.01[d]
18a[41]	A	OH	H	H	α	H	CH$_3$	>100	>100	7.34 ± 11.82	NT
20a	A	H	OH	H	β	H	CH$_3$	>100	>100	3.11 ± 2.58	>100
21a[41]	A	H	OH	H	α	H	CH$_3$	9.28 ± 0.04	11.20 ± 0.49	8.56 ± 9.00	NT
20b	A	H	OH	H	β	H	OCH$_3$	8.75 ± 0.49	95.77 ± 3.21	11.50 ± 5.66	NT
20c	A	H	OH	H	β	OCH$_3$	CH$_3$	>100	>100	1.49 ± 0.51	1.24[d]
21c	A	H	OH	H	α	OCH$_3$	CH$_3$	1.37 ± 0.14	>100	3.27 ± 0.09[d]	2.35 ± 1.11
23a	A	OH	OH	CH$_2$OH	β	H	CH$_3$	9.59 ± 0.42	11.07 ± 0.47	3.23 ± 3.76	4.58 ± 2.78
23b	A	OH	OH	CH$_2$OH	β	H	OCH$_3$	11.76 ± 0.06	14.34 ± 0.16	6.78 ± 2.25	17.94 ± 10.33
23c	A	OH	OH	CH$_2$OH	β	OCH$_3$	CH$_3$	9.45 ± 0.19	3.37 ± 0.06	4.66 ± 1.48	5.90 ± 2.58
25a	B	OH	OH	H	β	H	CH$_3$	12.46 ± 0.52	37.17 ± 1.68	3.65 ± 2.83	NT
25b	B	OH	OH	H	β	H	OCH$_3$	7.57 ± 1.05	11.73 ± 0.78	2.60 ± 1.51	10.64 ± 20.83
25c	B	OH	OH	H	β	OCH$_3$	CH$_3$	9.45 ± 0.19	3.37 ± 0.07	4.72 ± 1.48	9.56 ± 2.58
27a	B	OH	H		β	H	CH$_3$	>100	>100	NT	NT
28a	B	OH	H		α	H	CH$_3$	>100	>100	5.34 ± 4.76	NT
30a	B	H	OH		β	H	CH$_3$	35.24 ± 1.76	>100	3.72[d]	10.05 ± 6.75[d]
31a	B	H	OH		α	H	CH$_3$	>100	>100	4.96 ± 10.58	26.79 ± 58.24
33a	C	OH	OH		β	H	CH$_3$	2.38 ± 0.06	>100	>100	NT

[a] Values represent mean ± standard deviation for at least two separate experiments performed in triplicate. [b] Values represent mean ± standard deviation from dose response curves for at least two separate experiments performed in duplicate. [c] All error values listed represent 95% confidence intervals throughout the manuscript except where indicated. [d] Error values listed as standard deviations.

Table 2. Anti-proliferative Activity of Cyclohexyl Analogues

compd (IC$_{50}$, μM)	R^1	R^2	X	Y	SKBr3	MCF-7	LNCAP-LN3	PC3-MM2
43a	CH$_3$	CH$_3$	H	CH$_3$	>100[a]	>100[a]	1.24 ± 0.17[b,c]	2.49 ± 1.70[b]
43b	CH$_3$	CH$_3$	H	OCH$_3$	3.45 ± 1.73	1.56 ± 0.03	NT	NT
43c	CH$_3$	CH$_3$	OCH$_3$	CH$_3$	>100	>100	NT	NT
44a	H	CH$_3$	H	CH$_3$	>100	>100	1.14 ± 0.67	4.09 ± 1.63
44b	H	CH$_3$	H	OCH$_3$	6.38 ± 0.71	8.52 ± 0.36	NT	NT
44c	H	CH$_3$	OCH$_3$	CH$_3$	>100	>100	NT	NT
45[41]	H	H	H	CH$_3$	>100[a]	>100	1.58 ± 0.75	4.04 ± 0.38[c]
45b	H	H	H	OCH$_3$	7.44 ± 0.36	5.46 ± 0.36	NT	NT
45c	H	H	OCH$_3$	CH$_3$	8.18 ± 0.79	10.13 ± 1.04	NT	NT

[a] Values represent mean ± standard deviation for at least two separate experiments performed in triplicate. [b] Values represent mean ± standard deviation from dose response curves for at least two separate experiments performed in duplicate. [c] Error values listed as standard deviations.

In addition to the variable-sized sugar-containing analogues, cyclohexyl analogues were designed to examine if a sugar was necessary. Additionally, to probe the tolerance of steric bulk, analogues with and without alkyl substituents were pursued. Many of the simplified cyclohexyl sugar mimics were accessible using common procedures (Scheme 5) such as reduction with lithium aluminum hydride to produce compounds **37** and **38**, or Luche reduction to yield **39**. Compounds containing a double bond were designed to be coupled with the scaffold and subsequently oxidized to the corresponding diols (e.g., **43**−**45**).

Upon construction of the modified sugar analogues of novobiocin, the compounds were evaluated for anti-proliferative activity against SKBr3 (estrogen receptor negative, HER2 overexpressing breast cancer cells), MCF-7 (estrogen receptor positive breast cancer cells), LNCaP-LN3 (androgen-dependent human prostate cancer cells), and PC3-MM2 (androgen-independent prostate cancer cells) cell lines. As shown in Table 1, analogues containing six-membered pyranose moieties (scaffold **A**) were found to be the most active compounds against the two breast cancer cell lines. Analogues containing dihydroxyl groups consistently exhibited good to modest anti-proliferative activities against both breast cancer cell lines. In contrast, analogues that

contained a single hydroxyl at the 2′-position proved inactive, while most analogues with a 3′-hydroxyl exhibited modest activity. These data indicate that the 3′-position hydroxy group is essential for anti-proliferative activity. Interestingly, the natural substrate for the C-terminal pocket of Hsp90, ATP/ADP, also contains a 3′-hydroxyl. Although the β epimer exhibited better activity than its α counterpart (**14a**−**c** vs **15a**−**c**) for most analogues, this was not a general trend observed throughout the series (**20a**−**c** vs **21a**−**c**). In addition, the majority of the compounds from this series demonstrated modest activity against the prostate cancer cell lines. Notably, however, some compounds (**17a**) that were completely inactive against both breast cancer cells lines were efficacious against prostate cancer.

Analogues containing a cyclohexyl moiety in lieu of the sugar demonstrated a range of activities. While analogues containing an 8-methyl group (**43a**, **44a**, **45a**) were inactive against breast cancer, those with an 8-methoxy group (**43b**, **44b**, **45b**) exhibited an IC$_{50}$ value of ~10 μM, which is comparable to its noviosylated counterpart (Table 2).[33] Interestingly, the *gem*-dimethyl group is well tolerated in the case of the 8-methoxy coumarin (**43b**) but detrimental in the case of the 6-methoxy coumarin (**43c**). This finding suggests a mutually exclusive orientation between the *gem*-dimethyl group and substituents on the coumarin, which may preclude proper binding orientation.

Scheme 6. Retrosynthesis of Azasugar-Containing Biaryl Analogues
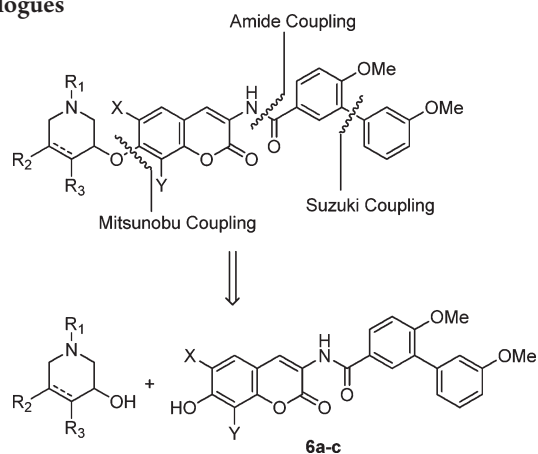
Scheme 8. Synthesis of 1,4-Azasugar Biaryl Analogues
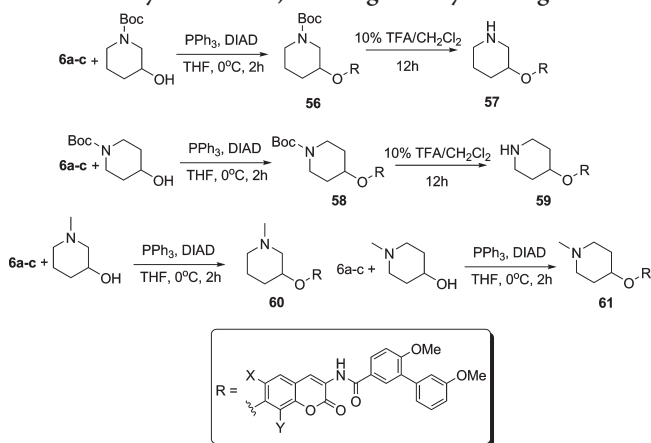
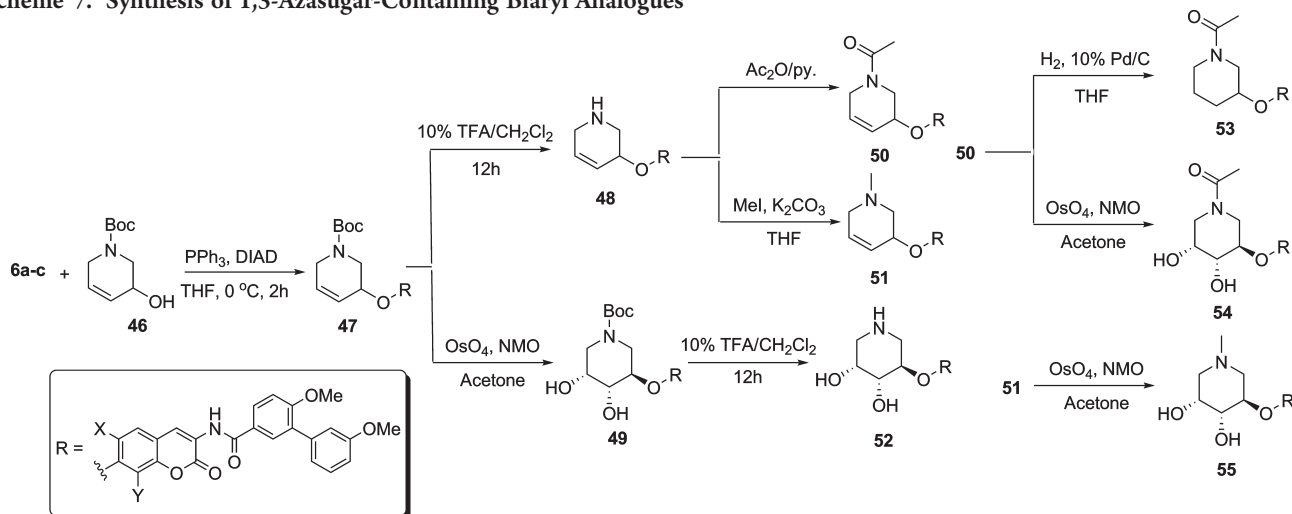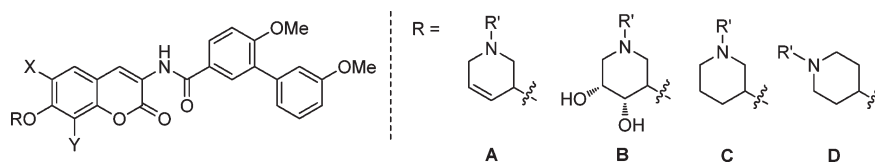**Scheme 7. Synthesis of 1,3-Azasugar-Containing Biaryl Analogues**

Table 3. Anti-proliferative Activity of Azasugar Analogues

compd (IC$_{50}$, μM)	R	X	Y	R′	SKBr3	MCF-7	LNCAP-LN3	PC3-MM2
48a	A	H	CH$_3$	H	1.61 ± 0.05^a	1.73^a	$4.27 \pm 0.05^{b,c}$	$4.40 \pm 0.06^{b,c}$
48b	A	H	OCH$_3$	H	3.07 ± 0.78	1.43 ± 0.37	6.45 ± 2.70^c	4.88 ± 2.20
48c	A	OCH$_3$	CH$_3$	H	1.21 ± 0.07	1.68 ± 0.04	5.40 ± 9.99	3.57 ± 0.71^c
50a	A	H	CH$_3$	Ac	>50	>50	0.90 ± 0.59	3.73 ± 0.67
51a	A	H	CH$_3$	CH$_3$	2.92 ± 1.33	5.29 ± 0.23	1.22^c	1.73 ± 1.80
51b	A	H	OCH$_3$	CH$_3$	3.42 ± 0.45	1.65 ± 0.28	0.36 ± 0.14	0.98 ± 0.40
51c	A	OCH$_3$	CH$_3$	CH$_3$	1.96 ± 0.48	5.27 ± 0.22	4.49 ± 0.17^c	3.87 ± 0.03^c
52a	B	H	CH$_3$	H	2.91 ± 0.90	2.07 ± 0.86	4.90 ± 9.16	6.33 ± 4.12
52b	B	H	OCH$_3$	H	8.98 ± 0.44	10.17 ± 0.02	12.19 ± 6.30	14.43 ± 7.39
52c	B	OCH$_3$	CH$_3$	H	3.65 ± 0.22	3.34	9.45 ± 5.90	6.84 ± 2.80
53a	C	H	CH$_3$	Ac	>50	>50	1.23 ± 0.67	3.42 ± 1.24
54a	B	H	CH$_3$	Ac	10.79 ± 0.08	9.18 ± 0.60	0.71 ± 0.54	2.22 ± 1.04
55a	B	H	CH$_3$	CH$_3$	3.92 ± 0.32	1.85 ± 0.02	0.59 ± 0.54	2.99 ± 1.27
55b	B	H	OCH$_3$	CH$_3$	6.64 ± 0.54	11.02 ± 1.12	1.50 ± 0.62	3.52 ± 1.43
55c	B	OCH$_3$	CH$_3$	CH$_3$	2.77 ± 0.90	2.01 ± 0.46	4.69 ± 0.57^c	4.17 ± 0.16^c
57a	C	H	CH$_3$	H	1.16 ± 0.16	1.63 ± 0.28	3.02 ± 0.97^c	2.57 ± 1.13
57b	C	H	OCH$_3$	H	2.61 ± 0.37	3.29 ± 0.42	12.72 ± 3.25	10.43 ± 2.15
57c	C	OCH$_3$	CH$_3$	H	2.27 ± 0.61	2.90 ± 0.67	3.66^c	2.59 ± 13.91
59a	D	H	CH$_3$	H	1.19 ± 0.06	1.47 ± 0.02	3.38 ± 1.25	4.12 ± 1.29
59b	D	H	OCH$_3$	H	1.79	3.23 ± 0.20	10.85 ± 5.92	8.47 ± 4.28
59c	D	OCH$_3$	CH$_3$	H	1.20 ± 0.08	2.82 ± 1.10	5.27 ± 22.18	4.02 ± 2.13
60a	C	H	CH$_3$	CH$_3$	2.06 ± 0.57	5.04 ± 0.02	1.22 ± 0.17^c	4.23 ± 1.68
60b	C	H	OCH$_3$	CH$_3$	1.40 ± 0.14	1.38 ± 0.14	1.78 ± 0.80	2.16 ± 1.28
60c	C	OCH$_3$	CH$_3$	CH$_3$	1.49 ± 0.06	1.41 ± 0.13	10.48 ± 5.46^c	6.86 ± 2.92^c
61a[41]	D	H	CH$_3$	CH$_3$	1.34 ± 0.18	1.51 ± 0.24	4.12 ± 0.16^c	3.13 ± 0.67
61b	D	H	OCH$_3$	CH$_3$	0.97 ± 0.07	1.39 ± 0.28	4.75 ± 2.03	3.71 ± 1.27
61c	D	OCH$_3$	CH$_3$	CH$_3$	1.19 ± 0.17	1.79 ± 0.09	4.17 ± 0.15^c	2.84 ± 1.88

^{a} Values represent mean ± standard deviation for at least two separate experiments performed in triplicate. ^{b} Values represent mean ± standard deviation from dose response curves for at least two separate experiments performed in duplicate. ^{c} Error values listed as standard deviations.

Scheme 9. Synthesis of Alkyl Sugar Biaryl Analogues
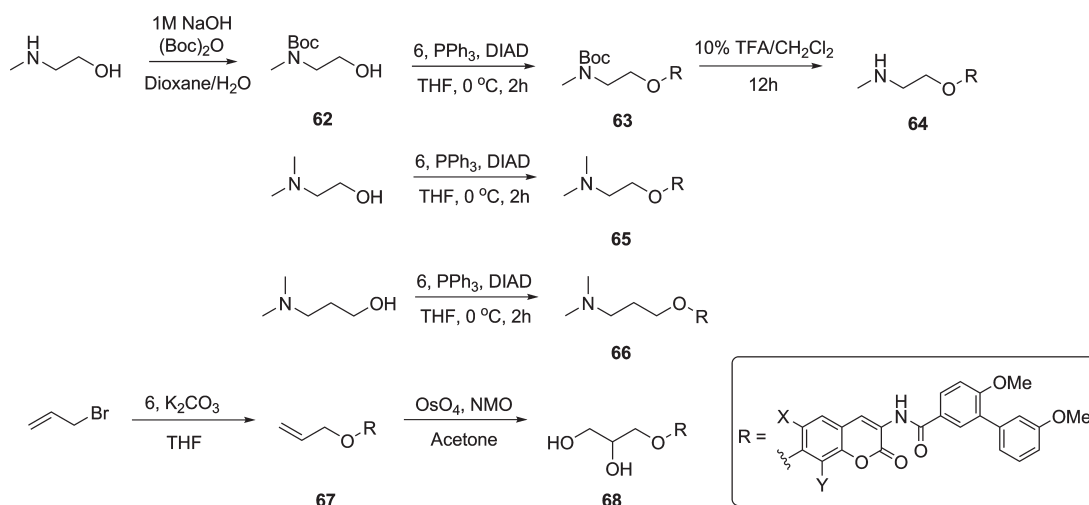
Overall, this library containing sugar surrogates and cyclohexyl groups confirmed the 3′-hydroxy as the most important functional group. Moreover, the 4′-methoxy, 5′-*gem*-dimethyl and anomeric oxygen found in noviose were identified as dispensable moieties. Several analogues (**15b**, **24c**, and **37a**) exhibited low micromolar anti-proliferative activity against SKBr3 cells, which makes them ∼500-fold more active than novobiocin.

Design, Synthesis, and Biological Evaluation of Azasugar Analogues of Novobiocin. After evaluation of the initial library, it was proposed that other six-membered heteroatom-containing ring systems may serve as replacements for noviose. *N*-Heterocycles are found in a wide variety of biologically active compounds, imparting solubility to otherwise insoluble aglycons. Several heterocycles were designed to probe hydrogen-bonding interactions with the binding pocket as well as to improve solubility.

In modular fashion, the analogues were assembled similarly to those described previously, allowing sequential coupling of various sugar surrogates and the biaryl side chain. As shown in the retrosynthetic analysis depicted in Scheme 6, the biaryl acid chloride, prepared from the corresponding biaryl acid, was coupled with coumarin **9**. Following deprotection, coumarin phenol **6** was etherified using Mitsunobu conditions to yield the desired analogues.

To avoid synthetic complications, only a single hydroxyl group was installed on the piperidine ring prior to Mitsunobu coupling and the amine was masked as the carbamate, **46**. With compound **6** and **46** in hand, compound **47** was synthesized via Mitsunobu etherification, followed by deprotection to yield amine **48** in quantitative yield. Acetylation of **48** gave amide **50**, while treatment with methyl iodide furnished the tertiary amine, **51**, which underwent dihydroxylation with OsO_4/NMO to give **55**. Dihydroxylation of **47** afforded compound **49**, which, upon removal of Boc, afforded **52**. Compounds **53** and **54** were synthesized from compound **50** via reduction or dihydroxylation conditions, respectively (Scheme 7).

In addition, compounds lacking the diol functionality and containing a transposed nitrogen within the heterocycle were selected for investigation. Boc-protected 1,3- or 1,4-azasugars were coupled with phenol **6** to afford compounds **56** and **58**, which were subsequently deprotected to yield amines **57** and **59**. Similarly, *N*-methylated analogues **60** and **61** were synthesized via Mitsunobu etherification with commercially available piperidines in good yields (Scheme 8).

Upon construction of the azasugar-containing analogues, they were evaluated for anti-proliferative activity against two breast and two prostate cancer cell lines. As shown in Table 3, the activity against breast cancer cells exhibited by the majority of

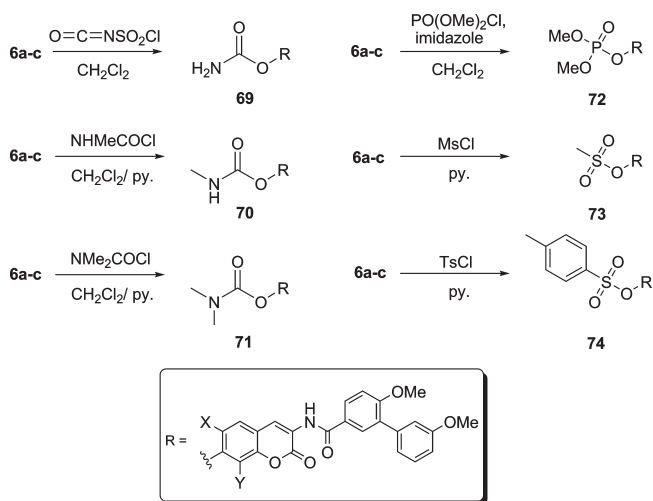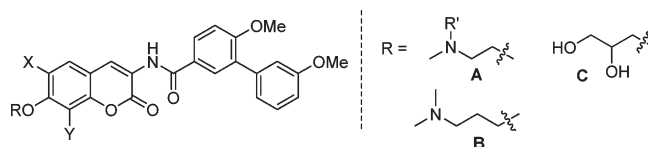**Scheme 10. Synthesis of Non-Sugar Biaryl Analogues**

Table 4. Anti-proliferative Activity of Novobiocin Analogues with Aliphatic Sugar Replacement

compd (IC_{50}, μM)	R	X	Y	R′	SKBr3	MCF-7	LNCAP-LN3	PC3-MM2
64a	A	H	CH_3	H	5.36 ± 0.08^a	9.80 ± 0.11^a	$>100^b$	$14.01 \pm 0.28^{b,c}$
64b	A	H	OCH_3	H	3.60 ± 0.28	4.32 ± 0.32	15.24 ± 7.96	9.12 ± 5.92
64c	A	OCH_3	CH_3	H	3.15 ± 0.54	6.23 ± 0.14	>100	11.77 ± 5.94
65a	A	H	CH_3	CH_3	1.02 ± 0.13	1.46 ± 0.08	6.65 ± 12.43	4.17 ± 19.64
65b	A	H	OCH_3	CH_3	1.77 ± 0.12	3.08 ± 0.08	5.22 ± 3.25	6.20 ± 2.22
65c	A	OCH_3	CH_3	CH_3	1.42 ± 0.21	1.29 ± 0.17	6.28 ± 2.22^c	4.87 ± 2.91
66a	B	H	CH_3		0.60 ± 0.01	0.50 ± 0.03	37.51 ± 54.24	12.85 ± 11.42
66b	B	H	OCH_3		0.91 ± 0.14	1.53 ± 0.14	8.03 ± 7.93	4.08 ± 1.83
66c	B	OCH_3	CH_3		0.49 ± 0.20	0.70 ± 0.15	4.71 ± 0.21^c	5.40 ± 3.15
68a	C	H	CH_3		>50	>50	NT	0.19 ± 0.33
68b	C	H	OCH_3		>50	>50	0.96 ± 1.20	1.66 ± 6.05
68c	C	OCH_3	CH_3		19.36 ± 2.45	20.47 ± 5.54	NT	NT

[a] Values represent mean ± standard deviation for at least two separate experiments performed in triplicate. [b] Values represent mean ± standard deviation from dose response curves for at least two separate experiments performed in duplicate. [c] Error values listed as standard deviations.

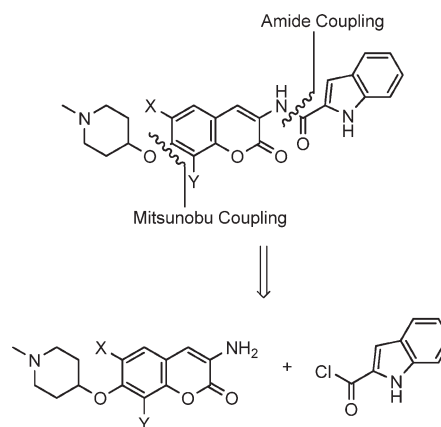**Table 5. Anti-proliferative Activity of Non-Sugar Analogues**
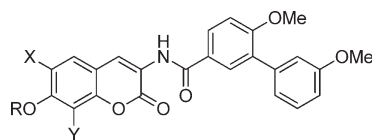
compd (IC$_{50}$, μM)	X	Y	R	SKBr3	MCF-7	LNCAP-LN3	PC3-MM2
6a[41]	H	CH$_3$	H	8.88 ± 0.48^a	6.93 ± 0.48^a	3.21 ± 1.78^b	5.36 ± 2.71^b
12a[41]	H	CH$_3$	COCH$_3$	0.98 ± 0.02	1.40	1.50 ± 1.00	2.85 ± 1.66
85[32]	H	CH$_3$	Noviose	7.50 ± 0.80	18.70 ± 1.44	NT	NT
73a[41]	H	CH$_3$	Ms	7.33 ± 0.96	8.85 ± 0.88	19.96 ± 42.67	>100[41]
74a[41]	H	CH$_3$	Ts	>100	>100	0.58 ± 1.34	>100
69a	H	CH$_3$	CONH$_2$	3.02 ± 0.56	1.16 ± 0.08	2.61 ± 1.09	6.37 ± 4.31
70a[41]	H	CH$_3$	CONHMe	2.40 ± 0.16	1.72 ± 0.16	3.75 ± 0.76	5.22 ± 2.16
71a	H	CH$_3$	CONMe$_2$	39.85 ± 0.48	74.35 ± 3.92	5.40 ± 6.58	>100
72a	H	CH$_3$	PO(OMe)$_2$	>100	>100	3.65 ± 5.73	>100
6b	OCH$_3$	CH$_3$	H	3.23 ± 1.20	11.70 ± 1.92	15.79 ± 32.60	11.23 ± 30.70
12b	OCH$_3$	CH$_3$	COCH$_3$	5.72 ± 0.02	1.50 ± 0.24	1.05 ± 0.59	1.69 ± 2.05
86[33]	OCH$_3$	CH$_3$	Noviose	58.80 ± 1.04	>100	26.57 ± 67.44	>100
73b	OCH$_3$	CH$_3$	Ms	>100	>100	>100	NT
74b	OCH$_3$	CH$_3$	Ts	>100	>100	NT	>100
69b	OCH$_3$	CH$_3$	CONH$_2$	6.83 ± 0.24	6.29 ± 0.88	3.55 ± 3.44	2.62 ± 2.04
70b	OCH$_3$	CH$_3$	CONHMe	1.53 ± 0.16	7.78 ± 1.68	4.77 ± 8.37	3.13 ± 2.34
71b	OCH$_3$	CH$_3$	CONMe$_2$	6.17 ± 1.68	34.4 ± 7.20	12.75 ± 0.32^c	4.04 ± 16.68
72b	OCH$_3$	CH$_3$	PO(OMe)$_2$	26.48 ± 0.80	24.22 ± 2.40	1.36 ± 2.80	31.32 ± 54.87
6c	H	OCH$_3$	H	>100	5.32 ± 0.08	6.18 ± 7.43	>100
12c	H	OCH$_3$	COCH$_3$	20.50 ± 1.28	8.62 ± 2.00	14.62 ± 23.63	19.33 ± 50.90
87[33]	H	OCH$_3$	Noviose	13.90 ± 0.96	9.00 ± 4.32	0.11 ± 0.02	1.44 ± 0.32
73c	H	OCH$_3$	Ms	>100	>100	0.87 ± 1.32	NT
74c	H	OCH$_3$	Ts	>100	>100	0.11 ± 4.68	NT
69c	H	OCH$_3$	CONH$_2$	76.83 ± 1.84	5.56 ± 0.24	4.83 ± 3.87	>100
70c	H	OCH$_3$	CONHMe	>100	6.54 ± 1.84	2.37 ± 1.44	1.68 ± 1.89
71c	H	OCH$_3$	CONMe$_2$	>100	>100	15.73 ± 14.09	11.57 ± 10.04
72c	H	OCH$_3$	PO(OMe)$_2$	18.07 ± 2.88	>100	6.58 ± 4.14	11.46 ± 6.54

^{a} Values represent mean ± standard deviation for at least two separate experiments performed in triplicate. ^{b} Values represent mean ± standard deviation from dose response curves for at least two separate experiments performed in duplicate. ^{c} Error values listed as standard deviations.

these secondary and tertiary amines varied between 1 and 3 μM, making them ~700-fold more active than novobiocin. Although dihydroxylation of the piperidine ring is well-tolerated when appended to the 8-methyl scaffold (52a), this is not the case for the other two scaffolds (52b and 52c). These data suggest that dihydroxylation of the piperidine ring is not essential for anti-proliferative activity. Inclusion of unsaturation within the piperidine ring is also well tolerated (scaffold A vs C and D, Table 3), while methylation of the amine within this unsaturated ring decreases activity (48 vs 51). It was observed that acetylation of the amine functionality (50a, 53a, 54a) severely decreased solubility and produced inactive compounds. Although insolubility can be overcome through dihydroxylation of the piperidine ring (54a), the resulting compound is ~5-fold less active than secondary or tertiary amines. There is no significant effect when the nitrogen is transposed within the piperidine ring, as all of the analogues exhibited activity between ~1–3 μM. In addition, piperidine compounds exhibited comparable activity to

Scheme 11. Retrosynthesis of Azasugar Indole Novobiocin Analogues

methylated piperidine compounds (**57** vs **60**, **59** vs **61**). Overall, these azasugar analogues consistently exhibited low micromolar anti-proliferative activity, representing an improved sugar mimic.

Design, Synthesis, and Biological Evaluation of Novobiocin Analogues with Acyclic Sugar Replacements. The promising results obtained when azasugars were appended to these scaffolds encouraged the synthesis of acyclic nitrogen-containing replacements. To probe the importance of a constrained ring system, a library of ring-opened, amine-containing sugar surrogates was designed. A series of heteroatom-containing aliphatic chains were synthesized to impart flexibility and explore the potential of additional interactions with the binding pocket. Aliphatic amines, either commercially available or prepared over a modest number of steps, were appended to coumarin core **6** through standard Mitsunobu coupling to yield compounds **64−66**. The dihydroxylated aliphatic chain was attached via treatment with allyl bromide followed by dihydroxylation to afford compound **68** (Scheme 9).

In addition to the aliphatic amine analogues synthesized, several simplified nonsugar molecules were appended in lieu of the noviose sugar. These nonsugars represent simplified functionalities manifested by compound **4**,[30] a recently described inhibitor of the Hsp90 C-terminus (Figure 2).[30] Substitutions were selected to probe hydrogen-bonding interactions, dimensions, and improve solubility. Carbamates (**69−71**) with variable substitution were prepared through standard conditions. Phosphate ester **71** was introduced through an esterification reaction to increase the hydrophilicity of the inhibitor, and finally, methyl and toluene sulfonic esters (**73**, **74**) were incorporated using the corresponding sulfonic chlorides to explore both the hydrogen bonding network and dimensions of the pocket similarly to that reported by Renoir and co-workers[34] (Scheme 10).

Upon construction of these alkyl and nonsugar compounds, they were evaluated for anti-proliferative activity against various cancer cell lines. The anti-proliferative data are summarized in Tables 4 and 5. All of the tertiary amine analogues demonstrated notable anti-proliferative activity of ∼1 μM, while the secondary amine analogues maintained activity of ∼3−5 μM against both breast cancer cell lines. The tertiary amine analogues homologated by two methylene groups (**65a−c**) exhibited activity of 1−3 μM, which is comparable to the piperidine analogues. Moreover, homologation by three methylene groups (**66a−c**) resulted in compounds that manifested anti-proliferative activity in the mid-nanomolar range, a finding that is consistent with the piperidine ring analogues. In contrast, the diol-containing analogues, when appended to the 8-methyl (**68a**) or 8-methoxy (**68b**) coumarin scaffolds were inactive but resulted in modest activity when appended to the 6-methoxy coumarin (**68c**). Furthermore, the aliphatic amine and corresponding dihydroxylated analogues manifested modest activities against the prostate cancer cell lines as well.

The anti-proliferative data for the nonsugar analogues revealed several interesting trends. The free phenol of each scaffold was nearly equal in activity to its noviosylated counterpart. Moreover, the acetylated phenols, in the case of the 8-methyl and 6-methoxy coumarins, displayed activities of ∼1 μM against breast cancer cells. Similarly, the carbamate and methylated carbamate were well tolerated when appended to 8-methyl and 6-methoxy coumarins, resulting in low micromolar analogues. Addition of another methyl group to the carbamate severely compromised activity. The methyl sulfonic ester was only tolerated when
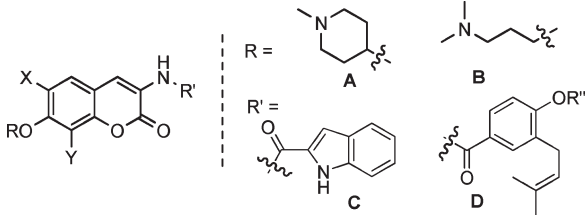
Scheme 12. Synthesis of Optimized Compounds
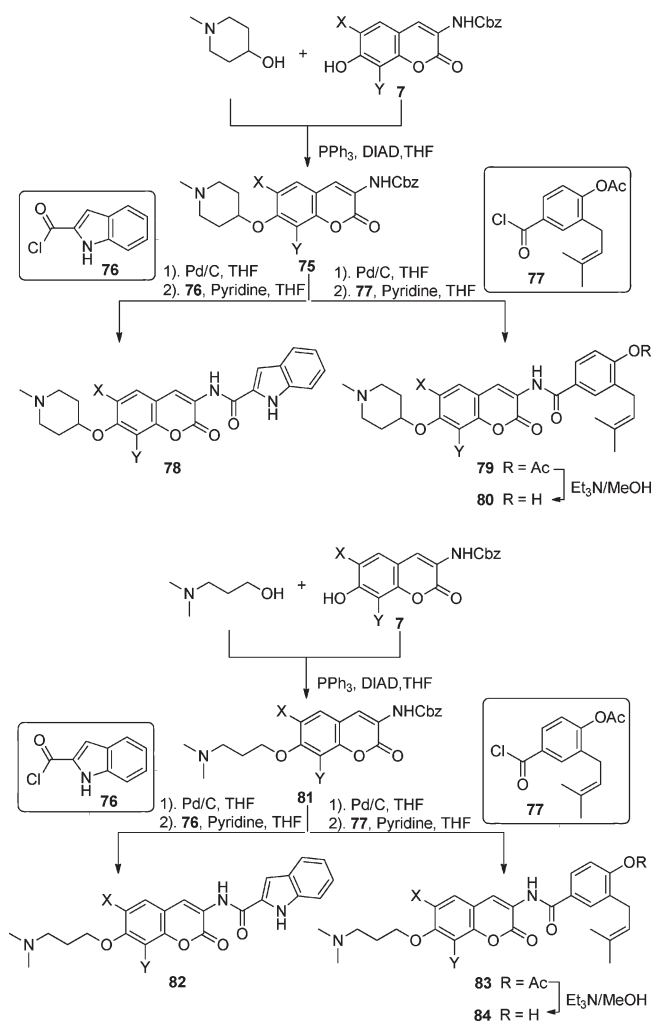
appended to the 8-methyl scaffold, while the toluene sulfonic ester was not tolerated by any analogue. Likewise, addition of the phosphate ester decreased activity of the analogues. Overall, hydrogen bonding and limited hydrophobic bulk are essential features for optimal binding.

Synthesis of Optimized Scaffolds Using Most Promising Noviose Replacements. On the basis of the biological evaluation discussed thus far, we identified the N-methyl-4-hydroxy-piperidine and 3-(dimethylamino)propan-1-ol as optimal noviose replacements. Therefore, these surrogates were appended to three previously identified and optimized coumarin scaffolds, containing either the 2-indole or prenylated benzamide side chain in lieu of the biaryl system.[32,42] As detailed earlier, the analogues were assembled in a modular fashion, allowing sequential coupling of sugar mimics and the indole acid chloride or benzoic acid chloride with the desired scaffold (Scheme 11). Unlike previously discussed scaffolds, the Mitsunobu ether coupling was performed prior to amide coupling due to solubility issues arising from the indole-containing free phenol.

As seen in Scheme 12, phenol **7**[32,33] was coupled with the azasugar using Mitsunobu conditions to yield protected scaffold **75**. The vinylogous amide was liberated via hydrogenolysis and coupled with indole acyl chloride **76**, which was generated from

Table 6. Anti-proliferative Activity of Optimized Analogues

compd (IC$_{50}$, μM)	R	X	Y	R'	R''	SKBr3	MCF-7	LNCAP-LN3	PC3-MM2
78a	A	H	CH$_3$	C		0.48 ± 0.09[a]	0.57 ± 0.03[a]	11.83 ± 0.54[b]	11.40 ± 5.25[b]
78b	A	H	OCH$_3$	C		2.58 ± 0.28	1.86 ± 0.08	12.64 ± 0.32[c]	7.93 ± 4.18
78c	A	OCH$_3$	CH$_3$	C		0.11 ± 0.01	0.52 ± 0.04	1.47 ± 0.53	0.87 ± 0.46
79a	A	H	CH$_3$	D	Ac	0.58 ± 0.04	1.18 ± 0.16	NT	2.12 ± 3.32
79b	A	H	OCH$_3$	D	Ac	1.07 ± 0.14	1.64 ± 0.24	NT	3.98 ± 0.06[c]
79c	A	OCH$_3$	CH$_3$	D	Ac	0.42 ± 0.01	0.58 ± 0.02	NT	1.41 ± 0.04[c]
80a	A	H	CH$_3$	D	H	0.76 ± 0.14	1.09 ± 0.08	NT	1.37 ± 1.42
80b	A	H	OCH$_3$	D	H	0.92 ± 0.01	1.54 ± 0.21	NT	3.53 ± 0.01[c]
80c	A	OCH$_3$	CH$_3$	D	H	0.42 ± 0.01	0.54 ± 0.02	NT	2.26 ± 1.43
82a	B	H	CH$_3$	C		1.13 ± 0.01	5.23 ± 0.22	NT	13.69 ± 0.18[c]
82b	B	H	OCH$_3$	C		1.50 ± 0.13	1.41 ± 0.09	4.71 ± 1.23[c]	8.95 ± 6.11
82c	B	OCH$_3$	CH$_3$	C		0.57 ± 0.09	0.56	NT	2.58 ± 4.47
83a	B	H	CH$_3$	D	Ac	0.46 ± 0.15	1.18 ± 0.02	NT	1.42 ± 0.05[c]
83b	B	H	OCH$_3$	D	Ac	0.78 ± 0.17	2.14 ± 0.22	NT	4.59 ± 4.23
83c	B	OCH$_3$	CH$_3$	D	Ac	0.36 ± 0.03	0.70 ± 0.03	NT	1.46 ± 0.03[c]
84a	B	H	CH$_3$	D	H	0.44 ± 0.02	1.35 ± 0.30	NT	1.81 ± 1.22
84b	B	H	OCH$_3$	D	H	0.77 ± 0.08	3.26 ± 0.26	NT	9.24 ± 17.79
84c	B	OCH$_3$	CH$_3$	D	H	0.39 ± 0.06	0.80 ± 0.07	NT	1.38 ± 0.02[c]

[a] Values represent mean ± standard deviation for at least two separate experiments performed in triplicate. [b] Values represent mean ± standard deviation from dose response curves for at least two separate experiments performed in duplicate. [c] Error values listed as standard deviations.

commercially available indole acid, to yield **78**.[32] The analogues containing a prenylated benzamide side chain (**77**) were assembled via the same sequence (Scheme 12), to yield alkyl amine analogues **79** and **80**. The prenylated side chain, **77**, was assembled as described previously by Burlison and co-workers.[29]

These compounds were evaluated for their anti-proliferative activity. The piperidine-containing analogues with an indole side chain (**78a**−**c**) exhibited increased anti-proliferative activity when attached to the 8-methyl and 6-methoxy coumarin (**78a** and **78c**) (Table 6). **78c** was notably 10-fold more active against SKBr3 cells when compared to its biaryl counterpart **61c**. In contrast, attachment of this sugar surrogate to the 8-methoxy coumarin (**78b**) compromised its activity versus the biaryl-containing analogue **61b**. In the case of the prenylated benzamide side chain (**79a**−**c** and **80a**−**c**), attachment of the azasugar increased activity against both cell lines, with the 6-methoxy coumarin manifesting superior activity (**79c** and **80c**). In addition, the intermediate acetylated phenols **79a**−**c** demonstrated comparable activity to the hydrolyzed phenol products **80a**−**c**. On the basis of the results obtained with the biaryl containing analogues, it was proposed that appendage of the aliphatic amine to the coumarins with an indole side chain would result in increased activity (see Table 4). However, the anti-proliferative activity of these indole analogues (**82a**−**c**) was maintained or slightly decreased in nearly every case. When these alkyl sugars were attached to the coumarins containing a prenylated benzamide side chain, the compounds manifested anti-proliferative activity in the mid-nanomolar range against SKBr3 cells. Moreover, compounds

built upon the 6-methoxy coumarin scaffold (**83c** and **84c**) exhibited the best activity against both cell lines.

Finally, several analogues from each of the libraries were selected for testing against a panel of melanoma and head and neck squamous cell carcinoma cell lines. In preliminary studies, C-terminal Hsp90 inhibitors have demonstrated modest activity against melanoma cells and have shown promise in treating head and neck cancers as well. Unpublished in vivo data produced by the Cohen lab has demonstrated tumor regression upon sustained treatment with a C-terminal Hsp90 inhibitor previously synthesized.[33] Analogues were selected that exhibited diverse structural features to probe the efficacy of these analogues against these cancers. B16F10 (murine melanoma), SKMEL28 (human melanoma), MDA1986 (human head and neck squamous cell carcinoma (HNSCC)), and JMAR (human oral squamous cell carcinoma) were selected for this panel of testing. The majority of the analogues tested manifested mid to low micromolar activity against these cell lines. While some of the compounds exhibited better activity against melanoma than head and neck cancers (**61b**), others were potent in a specific melanoma (**57b**) or a specific head and neck (**17a**) cell line (Table 7). The low micromolar activity of **78c** and **82c** against all of the cell lines warrant further investigation.

Validation of Hsp90 Inhibition via Western Blot Analysis. To confirm that the anti-proliferative activities exhibited by the optimized sugar analogues result from Hsp90 inhibition, analogues **80c** and **83c** were evaluated by Western blot analyses (Figure 7). Notably, compounds **61a**, **12b**, **70a**, and **87** have already been shown to exert their anti-proliferative activities

Table 7. Anti-proliferative Activity of Selected Analogues against Melanoma and HNSCC

compd (IC$_{50}$, μM)	B16F10	SKMEL28	MDA1986	JMAR
6b	5.77 ± 0.96 [a]	12.40 ± 0.64 [a]	6.70 ± 1.20 [a]	24.60 ± 1.92 [a]
12a	2.30 ± 0.32	2.14 ± 0.08	1.67 ± 0.16	12.60 ± 0.40
14a	37.50 ± 6.56	14.90 ± 2.88	13.40 ± 4.24	2.79 ± 0.64
15a	8.56 ± 2.16	15.80 ± 0.48	3.70 ± 0.64	6.14 ± 1.28
17a	1.01 ± 0.48	1.47 ± 0.24	0.81 ± 0.40	16.10 ± 2.16
18a	10.40 ± 1.20	19.60 ± 2.48	18.80 ± 3.68	3.60 ± 0.40
23a	9.60 ± 1.12	10.65 ± 0.40	5.70 ± 0.56	5.80 ± 1.04
25a	4.55 ± 1.20	5.74 ± 2.08	1.94 ± 0.40	12.64 ± 1.28
25b	1.30 ± 0.16	6.41 ± 0.56	5.73 ± 0.96	2.71 ± 0.32
27a	42.70 ± 3.36	18.40 ± 2.96	21.40 ± 3.12	14.90 ± 3.68
30a	12.70 ± 1.44	21.40 ± 3.28	6.90 ± 2.08	24.10 ± 3.28
31a	9.37 ± 1.04	12.40 ± 2.48	18.80 ± 3.76	6.19 ± 2.48
33a	>50	18.50 ± 5.76	22.90 ± 4.96	7.40 ± 1.68
40a	>50	23.80 ± 2.88	24.40 ± 2.00	6.70 ± 2.32
41a	>50	20.60 ± 2.16	21.80 ± 4.32	24.90 ± 2.80
42a	>50	18.60 ± 2.00	22.40 ± 3.36	7.50 ± 1.84
43a	15.90 ± 2.16	3.47 ± 1.20	18.80 ± 0.64	8.50 ± 1.68
44a	2.50 ± 0.48	11.41 ± 1.28	6.74 ± 2.08	2.73 ± 0.32
45a	14.10 ± 2.08	2.94 ± 1.20	17.90 ± 1.44	13.90 ± 2.00
48a	2.94 ± 0.08	5.41 ± 0.08	6.54 ± 0.56	3.40 ± 0.16
48b	3.41 ± 0.32	5.49 ± 1.12	5.97 ± 0.40	6.71 ± 0.24
48c	2.86 ± 0.24	5.41 ± 0.16	5.90 ± 0.40	11.60 ± 0.32
50c	21.40 ± 1.28	27.60 ± 1.20	25.10 ± 2.08	35.10 ± 1.20
51a	6.40 ± 1.92	10.79 ± 0.64	7.70 ± 0.56	11.40 ± 1.20
51b	6.47 ± 2.80	1.48 ± 0.48	2.36 ± 0.08	1.94 ± 0.16
51c	6.14 ± 0.64	31.50 ± 1.84	16.40 ± 1.68	18.40 ± 2.56
52a	2.80 ± 0.40	6.14 ± 1.28	5.60 ± 1.04	5.89 ± 0.48
52b	11.75 ± 0.40	11.40 ± 2.56	21.70 ± 1.12	11.60 ± 1.92
52c	5.04 ± 0.32	13.80 ± 2.56	13.80 ± 3.44	11.50 ± 0.72
53a	12.40 ± 2.00	20.9 ± 2.56	22.40 ± 1.36	15.14 ± 1.84
53c	23.90 ± 2.88	29.40 ± 3.36	36.40 ± 1.20	32.80 ± 3.36
55b	6.58 ± 0.48	5.90 ± 1.68	5.90 ± 0.48	6.70 ± 0.24
55c	2.81 ± 0.32	5.73 ± 0.32	12.80 ± 1.28	24.50 ± 0.72
57a	1.90 ± 0.24	2.79 ± 0.96	23.60 ± 2.88	>50
57b	0.64 ± 0.08	14.67 ± 0.40	12.80 ± 1.92	12.70 ± 1.44
57c	1.84 ± 0.08	7.19 ± 0.24	6.40 ± 0.96	5.70 ± 0.32
59a	2.76 ± 0.32	5.19 ± 0.16	2.74 ± 0.08	5.91 ± 0.40
59b	2.14 ± 0.08	16.45 ± 1.36	10.90 ± 0.64	12.60 ± 0.32
59c	1.84 ± 0.16	5.75 ± 0.24	14.60 ± 1.20	10.90 ± 0.48
60a	2.60 ± 0.32	6.14 ± 0.56	4.50 ± 0.08	12.60 ± 0.32
60b	1.51 ± 0.24	7.14 ± 0.40	11.40 ± 2.56	7.50 ± 0.64
60c	2.67 ± 0.32	5.86 ± 1.20	13.20 ± 0.72	19.10 ± 2.56
61b	0.41 ± 0.08	6.14 ± 0.32	13.10 ± 1.68	13.10 ± 0.64
61c	36.73 ± 0.64	3.74 ± 0.24	1.54 ± 0.08	1.84 ± 0.08
64a	37.40 ± 2.16	25.60 ± 2.96	21.90 ± 2.56	35.10 ± 2.16
65a	15.70 ± 4.56	14.70 ± 1.92	17.50 ± 3.28	18.40 ± 2.00
78c	1.19 ± 0.32	1.47 ± 0.08	1.42 ± 0.16	1.24 ± 0.24
82c	2.03 ± 0.08	1.35 ± 0.08	1.81 ± 0.32	2.65 ± 0.24

[a] Values represent mean ± standard deviation for at least two separate experiments performed in triplicate.

through an Hsp90-dependent mechanism, as confirmed through previously executed Western blot analyses.[30,33,41] It was essential

that these optimized derivatives demonstrate selective Hsp90-dependent client protein degradation, versus a loading control, to
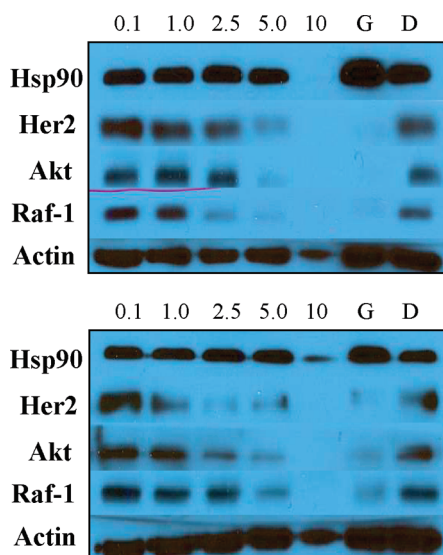
Figure 7. Western blot analyses of Hsp90 client protein degradation assays against MCF-7 cells. Concentrations (in μM) of **80c** (top) and **83c** (bottom) are indicated above each lane. G (geldanamycin, 500 nM) and D (DMSO) were respectively employed as positive and negative controls.

confirm the compounds reported herein also manifest Hsp90 inhibition. Figure 7 shows that in MCF-7 cells, the Hsp90-dependent client proteins Akt, Raf-1, and Her2 were degraded in a concentration-dependent manner upon treatment with the compounds. Hsp90 client protein degradation occurred at concentrations that paralleled the observed anti-proliferative IC_{50} values of 0.54 $\pm$ 0.03 μM for **80c** and 0.70 $\pm$ 0.04 μM for **83c**, confirming that Hsp90-dependent client protein degradation is causative for inhibition of cell growth. Furthermore, Hsp90 protein levels remained constant at all concentrations tested, which is consistent with C-terminal Hsp90 inhibition. Because the non-Hsp90-dependent protein, actin, was not affected by these analogues, it was concluded that selective degradation of Hsp90-dependent proteins occurred.

CONCLUSION

Several libraries of novobiocin analogues with various structural features were designed, synthesized, and evaluated. From the library of sugar mimics, we identified the pyranose as optimal and that a 2'-hydroxy group is indispensable. Several low micromolar analogues containing modified sugars were also identified. From the series of azasugar-containing analogues, we concluded that replacement of noviose with a piperidine ring resulted in consistent low micromolar anti-proliferative activities. The piperidine sugars confirmed that interactions made between noviose and the binding pocket could also be maintained with azasugars. In addition, the acyclic library produced several aliphatic sugar surrogates that manifested mid-nanomolar activity. This library confirmed that flexibility is tolerated and that noviose can be replaced with a simple acyclic moiety to maximize the potency of novobiocin analogues. Finally, the synthesis of optimized scaffolds with various cytotoxic benzamide side chains identified several novobiocin analogues that exhibited low nanomolar anti-proliferative activity. These analogues confirmed that results obtained from earlier studies could be applied to these appendages and produce compounds that warrant further study.

ASSOCIATED CONTENT

S **Supporting Information.** Experimental procedures and characterization for all compounds. This material is available free of charge via the Internet at http://pubs.acs.org.

AUTHOR INFORMATION

Corresponding Author
*Phone: (785) 864-2288. Fax: (785) 864-5326. E-mail: bblagg@ ku.edu.

Author Contributions
$^{\perp}$These authors contributed equally to this work

ACKNOWLEDGMENT

ABBREVIATIONS USED

Hsp90, 90 kDa heat shock protein; ATP, adenosine triphosphate; DNA, deoxyribonucleic acid; SAR, structure—activity relationships; Akt, protein kinase B; Her2, human epidermal growth factor receptor 2

REFERENCES

(1) Powers, M. V.; Workman, P. Targeting of multiple signalling pathways by heat shock protein 90 molecular chaperone inhibitors. *Endocr.-Relat. Cancer* **2006**, *13*, S125–S135.

(2) Maloney, A.; Workman, P. HSP90 as a new therapeutic target for cancer therapy: the story unfolds. *Expert Opin. Biol. Ther.* **2002**, *2*, 3–24.

(3) Sreedhar, A. S.; Kalmar, E.; Csermely, P.; Shen, Y. F. Hsp90 isoforms: functions, expression and clinical importance. *FEBS Lett.* **2004**, *562*, 11–15.

(4) Brandt, G. E. L.; Blagg, B. S. J. Alternative strategies of Hsp90 modulation for the treatment of cancer and other diseases. *Curr. Med. Chem.* **2009**, *9*, 1447–1461.

(5) Pratt, W. B.; Toft, D. O. Regulation of signaling protein function and trafficking by the hsp90/hsp70-based chaperone machinery. *Exp. Biol. Med.* **2003**, *228*, 111–133.

(6) Terasawa, K.; Minami, M.; Minami, Y. Constantly updated knowledge of Hsp90. *J. Biochem.* **2005**, *137*, 443–447.

(7) Buchner, J. Hsp90 & Co.—a holding for folding. *Trends Biochem. Sci.* **1999**, *24*, 136–141.

(8) Picard, D. Heat-shock protein 90, a chaperone for folding and regulation. *Cell. Mol. Life Sci.* **2002**, *59*, 1640–1648.

(9) Yonehara, M.; Minami, Y.; Kawata, Y.; Nagai, J.; Yahara, I. Heat-induced chaperone activity of Hsp90. *J. Biol. Chem.* **1996**, *271*, 2641–2645.

(10) Xiao, L.; Lu, X.; Ruden, D. M. Effectiveness of Hsp90 inhibitors as anti-cancer drugs. *Mini-Rev. Med. Chem.* **2006**, *6*, 1137–1143.

(11) Zhao, R.; Houry, W. A. Hsp90: a chaperone for protein folding and gene regulation. *Biochem. Cell Biol.* **2005**, *83*, 703.

(12) Issacs, J. S.; Xu, W.; Neckers, L. Heat shock protein 90 as a molecular target for cancer therapeutics. *Cancer Cell* **2003**, *3*, 213–217.

(13) Blagg, B. S. J.; Kerr, T. D. Hsp90 inhibitors: small molecules that transform the Hsp90 protein folding machinery into a catalyst for protein degradation. *Med. Res. Rev.* **2006**, *26*, 310–338.

(14) Peterson, L. B.; Blagg, B. S. J. To fold or not to fold: modulation and consequences of Hsp90 inhibition. *Future Med. Chem.* **2009**, *1*, 267–283.

(15) Workman, P. Combinatorial attack on multistep oncogenesis by inhibiting the Hsp90 molecular chaperone. *Cancer Lett.* **2004**, *206*, 149–157.

(16) Donnelly, A.; Blagg, B. S. Novobiocin and additional inhibitors of the Hsp90 C-terminal nucleotide-binding pocket. *Curr. Med. Chem.* **2008**, *15*, 2702–2717.

(17) Bishop, S. C.; Burlison, J. A.; Blagg, B. S. J. Hsp90: a novel target for the disruption of multiple signaling cascades. *Curr. Cancer Drug Targets* **2007**, *7*, 369–388.

(18) Lewis, R. J.; Tsai, F. T.; Wigley, D. B. Molecular mechanisms of drug inhibition of DNA gyrase. *BioEssays* **1996**, *18*, 661–671.

(19) Reece, R. J.; Maxwell, A. DNA gyrase: structure and function. *Crit. Rev. Biochem. Mol. Biol.* **1991**, *26*, 335–375.

(20) Laurin, P.; Ferroud, D.; Schio, L.; Klich, M.; Dupuis-Hamelin, C.; Mauvais, P.; Lassaigne, P.; Bonnefoy, A.; Musicki, B. Structure-activity relationship in two series of aminoalkyl substituted coumarin inhibitors of gyrase B. *Bioorg. Med. Chem. Lett.* **1999**, *9*, 2875–2880.

(21) Ali, J. A.; Jackson, A. P.; Howells, A. J.; Maxwell, A. The 43-kilodalton N-terminal fragment of the DNA gyrase B protein hydrolyzes ATP and binds coumarin drugs. *Biochemistry* **1993**, 32.

(22) Amolins, M. W.; Blagg, B. S. J. Natural product inhibitors of Hsp90: potential leads for drug discovery. *Mini-Rev. Med. Chem.* **2009**, *9*, 140–152.

(23) Holdgate, G. A.; Tunnicliffe, A.; Ward, W. H. J.; Weston, S. A.; Rosenbrock, G.; Barth, P. T.; Taylor, I. W. F.; Paupit, R. A.; Timms, D. The entropic penalty of ordered water accounts for weaker binding of the antibiotic novobiocin to a resistant mutant of DNA gyrase: a thermodynamic and crystallographic study. *Biochemistry* **1997**, *36*, 9663–9673.

(24) Lewis, R. J.; Singh, O. M. P.; Smith, C. V.; Skarzyknski, T.; Maxwell, A.; Wonacott, A. J.; Wigley, D. B. The nature of inhibition of DNA gyrase by the coumarins and the cyclothialidines revealed by X-ray crystallography. *EMBO J.* **1996**, *15*, 1412–1420.

(25) Tsai, F. T. F.; Singh, O. M. P.; Skarzynski, T.; Wonacott, A. J.; Weston, S.; Tucker, A.; Pauptit, R. A.; Breeze, A. L.; Poyser, J. P.; O'Brien, R.; Ladbury, J. E.; Wigley, D. B. The high-resolution crystal structure of a 24 kDa gyrase B fragment from *E. coli* complexed with one of the most potent coumarin inhibitors, clorobiocin. *Proteins* **1997**, *28*, 41–52.

(26) Marcu, M. G.; Schulte, T. W.; Neckers, L. Novobiocin and related coumarins and depletion of heat shock protein 90-dependent signaling proteins. *J. Natl. Cancer Inst.* **2000**, *92*, 242–248.

(27) Allan, R. K.; Mok, D.; Ward, B. K.; Ratajczak, T. Modulation of chaperone function and cochaperone interaction by novobiocin in the C-terminal domain of Hsp90. *J. Biol. Chem.* **2006**, *281*, 7161–7171.

(28) Yu, X. M.; Shen, G.; Neckers, L.; Blake, H.; Holzbeierlein, J.; Cronk, B.; Blagg, B. S. J. Hsp90 inhibitors identified from a library of novobiocin analogues. *J. Am. Chem. Soc.* **2005**, *127*, 12778–12779.

(29) Burlison, J. A.; Neckers, L.; Smith, A. B.; Maxwell, A.; Blagg, B. S. J. Novobiocin: redesigning a DNA gyrase inhibitor for selective inhibition of Hsp90. *J. Am. Chem. Soc.* **2006**, *128*, 15529–15536.

(30) Shelton, S. N.; Shawgo, M. E.; Comer, S. B.; Lu, Y.; Donnelly, A. C.; Szabla, K.; Tanol, M.; Vielhauer, G. A.; Rajewski, R. A.; Matts, R. L.; Blagg, B. S.; Robertson, J. D. KU135, a novel novobiocin-derived C-terminal inhibitor of Hsp90, exerts potent antiproliferative effects in human leukemic cells. *Mol. Pharmacol.* **2009**, *76*, 1314–1322.

(31) Burlison, J. A.; Blagg, B. S. J. Synthesis and evaluation of coumermycin A1 analogues that inhibit the Hsp90 protein folding machinery. *Org. Lett.* **2006**, *8*, 4855–4858.

(32) Burlison, J. A.; Avila, C.; Vielhauer, G.; Lubbers, D. J.; Holzbeierlein, J.; Blagg, B. S. J. Development of novobiocin analogues that manifest anti-proliferative activity against several cancer cell lines. *J. Org. Chem.* **2008**, *73*, 2130–2137.

(33) Donnelly, A. C.; Mays, J. R.; Burlison, J. A.; Nelson, J. T.; Vielhauer, G.; Holzbeierlein, J.; Blagg, B. S. J. The design, synthesis, and evaluation of coumarin ring derivatives of the novobiocin scaffold that exhibit antiproliferative activity. *J. Org. Chem.* **2008**, *73*, 8901–8920.

(34) Le Bras, G.; Radanyi, C.; Peyrat, J.-F.; Brio, J.-D.; Alami, M.; Marsaud, V.; Stella, B.; Renoir, J.-M. New novobiocin analogues as antiproliferative agents in breast cancer cells and potential inhibitors of heat shock protein 90. *J. Med. Chem.* **2007**, *50*, 6189–6200.

(35) Radanyi, C.; Le Bras, G.; Messaoudi, S.; Bouclier, C.; Peyrat, J.-F.; Brion, J.-D.; Marsaud, V.; Renoir, J.-M.; Alami, M. Synthesis and biological activity of simplified denoviose-coumarins related to novobiocin as potent inhibitors of heat-shock protein 90 (hsp90). *Bioorg. Med. Chem. Lett.* **2008**, *18*, 2495–2498.

(36) Yu, X. M.; Shen, G.; Blagg, B. S. J. Synthesis of (−)-noviose from 2,3-*O*-isopropylidene-D-erythronolactol. *J. Org. Chem.* **2004**, *69*, 7375.

(37) Hosmane, R. S.; Hong, M. How important is the N-3 sugar moiety in the tight-binding interaction of coformycin with adenosine deaminase? *Biochim. Biophys. Res. Commun.* **1997** *236*, 88–93.

(38) Eis, C.; Nidetzky, B. Substrate-binding recognition and specificity of trehalose phosphorylase from Schizophyllum commune examined in steady-state kinetic studies with deoxy and deoxyfluoro substrate analogues and inhibitors. *Biochem. J.* **2002**, *363*, 335–340.

(39) Werz, D. B.; Seeberger, P. H. Carbohydrates as the next frontier in pharmaceutical research. *Chemistry* **2005**, *11*, 3194–3206.

(40) Yu, Y. M.; Han, H.; Blagg, B. S. J. Synthesis of mono- and dihydroxylated furanoses, pyranoses, and an oxepananose for the preparation of natural product analogue libraries. *J. Org. Chem.* **2005**, *70*, 5599.

(41) Donnelly, A.; Zhao, H.; Kusuma, B. R.; Blagg, B. S. J. Cytotoxic sugar analogues of an optimized novobiocin scaffold. *MedChemComm* **2010**, *1*, 165–170.

(42) Zhao, H.; Kusuma, B. R.; Blagg, B. S. J. Synthesis and evaluation of noviose replacements on novobiocin that manifest antiproliferative activity. *ACS Med. Chem. Lett.* **2010**, *1*, 311–315.